HAL
open science

Characterization of the Amino Acids from Neisseria meningitidis MsrA Involved in the Chemical Catalysis of the Methionine Sulfoxide Reduction Step

Mathias Antoine, Adeline Gand, Sandrine Boschi-Muller, Guy Branlant

To cite this version:

Mathias Antoine, Adeline Gand, Sandrine Boschi-Muller, Guy Branlant. Characterization of the Amino Acids from Neisseria meningitidis MsrA Involved in the Chemical Catalysis of the Methionine Sulfoxide Reduction Step. Journal of Biological Chemistry, 2006, 281 (51), pp.39062-39070. 10.1074/jbc.M608844200 . hal-01690778

HAL Id: hal-01690778

https://hal.univ-lorraine.fr/hal-01690778v1

Submitted on 23 Jan 2018

HAL is a multi-disciplinary open access archive for the deposit and dissemination of scientific research documents, whether they are published or not. The documents may come from teaching and research institutions in France or abroad, or from public or private research centers.

L'archive ouverte pluridisciplinaire **HAL**, est destinée au dépôt et à la diffusion de documents scientifiques de niveau recherche, publiés ou non, émanant des établissements d'enseignement et de recherche français ou étrangers, des laboratoires publics ou privés.

THE JOURNAL OF BIOLOGICAL CHEMISTRY VOL. 281, NO. 51, pp. 39062–39070, December 22, 2006
© 2006 by The American Society for Biochemistry and Molecular Biology, Inc. Printed in the U.S.A.

Characterization of the Amino Acids from *Neisseria meningitidis* MsrA Involved in the Chemical Catalysis of the Methionine Sulfoxide Reduction Step*

Received for publication, September 13, 2006, and in revised form, October 18, 2006 Published, JBC Papers in Press, October 24, 2006, DOI 10.1074/jbc.M608844200

Mathias Antoine[1], **Adeline Gand**[1], **Sandrine Boschi-Muller, and Guy Branlant**[2]

From the Maturation des ARN et Enzymologie Moléculaire, Unite Mixte de Recherche, CNRS-UHP 7567, Nancy Université, Faculté des Sciences et Techniques, Bld des Aiguillettes, BP 239, 54506 Vandoeuvre-les-Nancy, France

Methionine sulfoxide reductases (Msrs) are ubiquitous enzymes that reduce protein-bound methionine sulfoxide back to Met in the presence of thioredoxin. *In vivo*, the role of the Msrs is described as essential in protecting cells against oxidative damages and as playing a role in infection of cells by pathogenic bacteria. There exist two structurally unrelated classes of Msrs, called MsrA and MsrB, specific for the *S* and the *R* epimer of the sulfoxide function of methionine sulfoxide, respectively. Both Msrs present a similar catalytic mechanism, which implies, as a first step, a reductase step that leads to the formation of a sulfenic acid on the catalytic cysteine and a concomitant release of a mole of Met. The reductase step has been previously shown to be efficient and not rate-limiting. In the present study, the amino acids involved in the catalysis of the reductase step of the *Neisseria meningitidis* MsrA have been characterized. The invariant Glu-94 and to a lesser extent Tyr-82 and Tyr-134 are shown to play a major role in the stabilization of the sulfurane transition state and indirectly in the decrease of the pK_{app} of the catalytic Cys-51. A scenario of the reductase step is proposed in which the substrate binds to the active site with its sulfoxide function largely polarized via interactions with Glu-94, Tyr-82, and Tyr-134 and participates via the positive or partially positive charge borne by the sulfur of the sulfoxide in the stabilization of the catalytic Cys.

Methionine sulfoxide reductases (Msr)[3] are enzymes that catalyze the reduction of free and protein-bound methionine sulfoxide (MetSO) back to Met. Two structurally unrelated classes of Msrs have been described so far. MsrAs are stereo specific toward the *S* isomer on the sulfur of the sulfoxide function, whereas MsrBs are specific toward the *R* isomer. Both classes share a similar three-step catalytic mechanism (Scheme 1). First, the reductase step leads to formation of a sulfenic acid intermediate on the catalytic cysteine concomitantly with the release of one mole of Met/mole of Msr. Then, an intra-disulfide bond is formed via the attack of a second Cys (called the recycling Cys) on the sulfenic acid intermediate accompanied by release of a water molecule. Finally, the disulfide bond is reduced by thioredoxin (Trx) in the last step. Recently, the kinetics of the three steps have been investigated for MsrA and MsrB domains of the PilB protein of *Neisseria meningitidis* (1, 2). For both classes of Msrs, the rate-limiting step is associated with the Trx recycling process, whereas the rate of formation of the intra-disulfide bond is governed by that of formation of the sulfenic acid intermediate, the rate of which is fast.

The three-dimensional structures of the MsrA from *Escherichia coli*, *Bos taurus,* and *Mycobacterium tuberculosis* have been recently solved by x-ray crystallography (3–5). The active site can be represented as an opened basin readily accessible to the MetSO substrate in which the catalytic Cys-51 is located at the entrance of the α 1 helix. In all the structures, the active site is occupied by a molecule that is covalently or non-covalently bound to the catalytic cysteine. In the case of *E. coli* MsrA, a dimethyl arsenate molecule is covalently bound, whereas it is a dithiothreitol molecule in *B. taurus* enzyme. In the case of *M. tuberculosis* MsrA, a methionine residue from a neighboring monomer occupies the active site. In all three structures, a water molecule is present, the position of which can mimic the oxygen atom of the sulfoxide function of MetSO. This water molecule is tightly H-bonded to three invariant amino acid residues, *i.e.* Tyr-82, Glu-94, and Tyr-134. All the three structures also support the involvement of invariant Phe-52 and Trp-53 in the substrate recognition via the formation of a hydrophobic pocket in which the ϵ methyl group of MetSO can bind.

Study of the reduction mechanism of dimethyl sulfoxide (Me_2SO) by methanethiol in Me_2SO solution has recently been investigated by quantum chemistry calculations (6). It was shown that 1) a sulfurane species is formed prior to formation of either a sulfenic acid intermediate or a disulfide species and 2) the rate-limiting step is governed by proton transfer between the thiol and the sulfoxide functions prior to sulfurane formation. Although these conclusions are derived from studies based on a model in solution, they provide a framework for the study of the chemical reductase step occurring within the MsrA active site.

In the present study, the role of Glu-94, Tyr-82, and Tyr-134 residues and how the catalytic Cys-51 is stabilized in the reductase step of the MsrA from *N. meningitidis* have been investi-

* This research was supported by the CNRS, the University of Nancy I, the Institut Federatif de Recherche 111 Bioingénierie, the Association pour la Recherche sur le Cancer (ARC-No 5436), and the French Ministry of Research (ACI BCMS047). The costs of publication of this article were defrayed in part by the payment of page charges. This article must therefore be hereby marked "*advertisement*" in accordance with 18 U.S.C. Section 1734 solely to indicate this fact.

[1] Supported by the French Ministry of Research.

[2] To whom correspondence should be addressed. Tel.: 33-3-83-68-43-04; Fax: 33-3-83-68-43-07; E-mail: Guy.Branlant@maem.uhp-nancy.fr.

[3] The abbreviations used are: Msr, methionine sulfoxide reductase; 2PDS, 2,2′-dipyridyl disulfide; AcMetSONHMe, Ac-L-Met-*R*,*S*-SO-NHMe; AcMetNHMe, Ac-L-Met-NHMe; Me_2SO, dimethyl sulfoxide; MetSO, methionine sulfoxide; pK_{app}, apparent p*K*a; Trx, thioredoxin.

Downloaded from http://www.jbc.org/ at CNRS on January 23, 2018

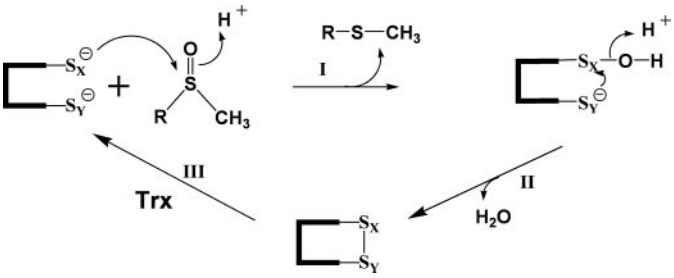

SCHEME 1. **Schematic representation of the catalytic mechanism of MsrA and MsrB from *N. meningitidis*.** The mechanism consists of three steps. In step 1, called the reductase step, a sulfenic acid intermediate is formed on the catalytic Cys-X with a concomitant release of one mol of Met/mol of enzyme. In step II, a disulfide bond is formed between the Cys-X and the recycling Cys-Y with a release of a water molecule. In step III, return of the active site to a fully reduced state proceeds via reduction of the Msr disulfide bond by reduced Trx. *RSOCH*$_3$ and *RSCH*$_3$ represent MetSO and Met, respectively. For *N. meningitidis* MsrA, Cys-X = Cys-51 and Cys-Y = Cys-198.

gated. For that, the kinetic parameters and the pH dependence of the rate constant of the reductase step of mutated MsrAs at positions 82, 94, and 134 were determined and compared with those of the wild type. The pK_{app} of Cys-51 in the free enzyme was also determined. The results show that Cys-51 is activated upon substrate binding to the active site with a shift of its pK_a from 9.5 to 5.7. Substitutions at positions 82, 94, and 134 do not modify the apparent affinity for the substrate in the reductase step. In contrast, drastic decrease of the reductase step rate is observed for the E94A and Y82F/Y134F MsrAs, whereas E94Q MsrA displays only a small decrease. Moreover, each mutated MsrA is characterized by a shift of the pK_{app} of its Cys-51 to higher values compared with wild type. Taking into account all the results, a scenario for the catalysis of the sulfoxide reductase step is proposed in which Glu-94, Tyr-82, and Tyr-134 stabilize the sulfurane transition state formed. In this scenario, the substrate binds to the active site with its sulfoxide function largely polarized via interactions with the side chains of Glu-94, Tyr-82, and Tyr-134 and plays a major role in stabilizing Cys-51 via the positive, or partially positive, charge borne by the sulfur of the sulfoxide function.

EXPERIMENTAL PROCEDURES

Site-directed Mutagenesis, Production, and Purification of Wild-type and Mutated N. meningitidis MsrAs—The *E. coli* strain used for all *N. meningitidis* MsrA productions was BE002 (MG1655 msrA::specΩ, msrB::α 3kana), transformed with the plasmidic construction pSKPILBMsrA containing only the coding sequence of *msrA* from *pilB*, under the *lac* promoter (7). The BE002 strain was kindly provided by Dr. F. Barras. Its use prevented expression of endogenous wild-type MsrA and MsrB from *E. coli* and thus avoided any contamination of the activity of the *N. meningitidis* MsrA by the Msrs from *E. coli*. Site-directed mutageneses were performed using the QuikChange site-directed mutagenesis kit (Stratagene).

Purifications were realized as previously described (1). Wild-type and mutated MsrAs were pure, as checked by electrophoresis on 12.5% SDS-PAGE gel followed by Coomassie Brilliant Blue R-250 staining and by electrospray mass spectrometry analyses. Storage of the enzymes was done as previously described. The molecular concentration was determined spectrophotometrically, using extinction coefficient at 280 nm of 26,200 $M^{-1}\cdot cm^{-1}$ for wild-type and mutated MsrAs. In this report, *N. meningitidis* MsrA amino acid numbering is based on *E. coli* MsrA sequence.

Quantification of the Free Cysteine Content with 5,5′-Dithiobis(2-nitro)benzoate—Cysteine content of MsrA was routinely determined using 5,5′-dithiobis(2-nitro)benzoate under non-denaturing conditions in buffer A (50 mM Tris-HCl, 2 mM EDTA, pH 8) as previously described (8).

pH Dependence of MsrA Thiol Reaction Rates with 2,2′-Dipyridyl Disulfide (2PDS)—Because of the high reactivity of Cys-51 and Cys-198 in MsrA, fast kinetic measurements were carried out on an Applied PhotoPhysics SX18MV-R stopped-flow apparatus. MsrA reactions with 2PDS were performed at 25 °C under pseudo-first-order conditions in 30 mM acetic acid, 30 mM imidazole, 120 mM Tris/HCl buffer at constant ionic strength of 0.15 M over a pH range of 6 to 10 (polybuffer B). MsrA and 2PDS concentrations after mixing were 6.2 and 310 μM, respectively. The pseudo-first-order rate constant k_{obs} was determined at each pH by fitting the absorbance (A) at 343 nm *versus* time (t) to mono-exponential Equation 1, where a is the burst amplitude and c is the end point. The second-order rate constants k_2 were calculated by dividing k_{obs} by 2PDS concentration and then fitted to Equation 2, in which k_{2max} represents the second rate constant for the thiolate form.

$$A = a(1 - e^{-k_{obs}t}) + c \qquad \text{(Eq. 1)}$$

$$k_2 = \frac{k_{2max}}{1 + 10^{(pK_a - pH)}} \qquad \text{(Eq. 2)}$$

Measurement of the Thiol Ionization by Ultraviolet Absorbance—Absorbance spectra were measured for all enzymes in 1.0-cm path length quartz cuvettes in a SAFAS UV-visible absorbance spectrophotometer. The protein samples were diluted to 23 μM in polybuffer B. Spectra were recorded at 25 °C in 0.5-nm steps from 300 to 200 nm over a pH range of 7 to 10. The buffer solution was scanned relative to air, followed by a protein solution in the same cuvette *versus* air. The two spectra were then subtracted and the difference converted to molar absorption coefficients at 240 nm ($\epsilon_{240\ nm}$). Data were fitted to a model derived from the Henderson-Hasselbach equation as shown in Equation 3 for one apparent pK_a.

$$\epsilon_{240\ nm} = \epsilon_{SH} + \frac{\epsilon_{S^-}}{1 + 10^{(pK_a - pH)}} \qquad \text{(Eq. 3)}$$

Steady-state MsrA Kinetics in the Presence of the Trx Recycling System—Steady-state kinetic parameters were determined with the Trx reductase recycling system (*E. coli* Trx (100 μM), *E. coli* Trx reductase (4.8 μM), NADPH (1.2 mM)) and by varying the concentrations of AcMetSONHMe. AcMetSONHMe was prepared and purified as previously described (2). Initial rate measurements were carried out at 25 °C in buffer A or polybuffer B on a Kontron Uvikon 933 spectrophotometer by following the decrease of the absorbance at 340 nm due to the oxidation of NADPH. Initial rate data were fitted to the Michaelis-Menten relationship using least squares analysis to determine k_{cat} and K_m for AcMetSONHMe. *E. coli* Trx1 and

Downloaded from http://www.jbc.org/ at CNRS on January 23, 2018

Trx reductase were prepared following experimental procedures already published (7).

Preparation of MsrA under Oxidized Disulfide State—MsrA oxidation was achieved by mixing 100 μM MsrA with 100 mM MetSO in buffer A. The MetSO used was DL-Met-*R,S*-SO of which only the *S* isomer is a substrate for MsrA. After 10 min of incubation at room temperature, oxidized proteins were passed through an Econo-Pac 10 DG desalting column (Bio-Rad) equilibrated with buffer A. Oxidation of MsrA in the disulfide state was checked by titration with 5,5′-dithiobis(2-nitro)benzoate.

Fluorescence Properties of Wild-type and Mutated MsrAs—The fluorescence excitation and emission spectra of wild-type and mutated MsrAs in their reduced and Cys-51/Cys-198 disulfide state were recorded on a flx spectrofluorometer (SAFAS) thermostated at 25 °C in buffer A with 10 μM of each protein as previously described (1).

Determination of the Rate of Met Formation and of Thiol Loss by Single Turnover Quenched Flow Experiments—Quenched flow measurements were carried out at 25 °C on a SX18MV-R stopped-flow apparatus (Applied PhotoPhysics) fitted for double mixing and adapted to recover the quenched samples as previously described (1). The apparatus worked in a pulsed mode. Under the conditions used, a minimum aging time of ~25–40 ms was determined. Equal volumes (57.5 μl) of a solution containing 550 μM Glu-94-mutated MsrA in buffer A and a solution containing AcMetSONHMe in buffer A were mixed in the aging loop. The mixture was then allowed to react for the desired time before being mixed with 115 μl of a quenched aqueous solution containing 2% of trifluoroacetic acid. Quenched samples were then collected in a 200-μl loop. For each aging time, four shots were done and the four corresponding quenched samples were pooled in a volume of 700 μl and then analyzed.

After protein precipitation and centrifugation, Ac-L-Met-NHMe (AcMetNHMe) quantification in the resulting supernatant was carried out by reverse phase chromatography as previously described (2): 100 μl were injected onto a 4.6 × 250-mm Atlantis dC18 reverse phase column (Waters) on an AKTA explorer system (Amersham Biosciences) equilibrated with H_2O/0.1% trifluoroacetic acid. AcMetNHMe was eluted after AcMetSONHMe with a linear gradient of acetonitrile.

The other part of the quenched samples that was not treated with 100% of trifluoroacetic acid was used to 1) determine the protein concentration from the absorbance at 280 nm and 2) quantify the free cysteine content, using 2PDS as a thiol probe, in the presence of urea to avoid precipitation of the protein in the cuvette. Progress curves of pyridine-2-thione production were recorded at 343 nm in 1.1 M urea, buffer A. Enzyme concentration was 6.19 μM, and 2PDS concentration was 665 μM. The amount of pyridine-2-thione formed was calculated using an extinction coefficient at 343 nm of 8,080 $M^{-1}\cdot cm^{-1}$.

Data were plotted as mole of AcMetNHMe formed/ mole of MsrA and as free remaining thiols/mole of MsrA, both as a function of time. The rate of Met formation was determined by fitting the curve to the monoexponential Equation 4 in which *a* represents the fraction of Met formed/mole of MsrA and k_{Met} represents the rate constant.

$$y = a(1 - e^{-k_{Met}t}) \quad \text{(Eq. 4)}$$

The rate of loss in free thiols was determined by fitting the curve to the monoexponential Equation 5 in which *y*0 represents the number of free remaining thiols, *a* the number of oxidized thiols, and k_{SS} the rate constant.

$$y = y0 + ae^{-k_{SS}t} \quad \text{(Eq. 5)}$$

Kinetics of the Formation of the Cys-51/Cys-198 MsrA Disulfide Bond in the Absence of Reductant by Single Turnover Stopped-flow Experiment at pH 8—Kinetics of the Trp-53 fluorescence variation associated with the formation of the Cys-51/Cys-198 disulfide bond were measured for E94Q, Y82F, and Y134F MsrAs at 25 °C on a SX18MV-R stopped-flow apparatus (Applied PhotoPhysics) fitted for fluorescence measurements as described previously (1). The excitation wavelength was set at 284 nm, and the emitted light was collected using a 320-nm cutoff filter. One syringe contained MsrA in buffer A (10 μM final concentration after mixing), and the other one contained AcMetSONHMe at various concentrations in buffer A. An average of at least six runs was recorded for each AcMetSONHMe concentration. Rate constants, k_{obs}, were obtained by fitting fluorescence traces with the monoexponential Equation 6 in which *c* represents the end point, *a* the amplitude of the fluorescence increase (<0), and k_{obs} the rate constant.

$$y = ae^{-k_{obs}t} + c \quad \text{(Eq. 6)}$$

Data were fitted to Equation 7 using least square analysis to determine k_{max} and K_S for AcMetSONHMe. *S* represents the AcMetSONHMe concentration and K_S the apparent affinity constant.

$$k_{obs} = \frac{k_{max}S}{K_S + S} \quad \text{(Eq. 7)}$$

Kinetics of the Trp-53 fluorescence variation associated with the formation of the Cys-51/Cys-198 disulfide bond were measured for Y82F/Y134F and Y82F/Y134F/E94Q MsrAs at 25 °C on a flx spectrofluorometer (SAFAS). The excitation wavelength was set at 284 nm, and the fluorescence emission at 340 nm was recorded *versus* time after enzyme addition. Data were then treated as described above to obtain k_{obs}, k_{max}, and K_S values.

pH Dependence of the Reductase Step Rate Constant—Determination of k_{max} and K_S as a function of pH was carried out for wild-type MsrA by single turnover pre-steady-state fluorescence stopped-flow spectroscopy, using the same procedure as described in the previous section but replacing buffer A with polybuffer B. k_{obs} values for E94Q, Y82F, Y134F, Y82F/Y134F, and Y82F/Y134F/E94Q MsrAs were determined at saturating concentration of AcMetSONHMe as a function of pH. Kinetics of Trp-53 fluorescence variation were recorded either with the stopped-flow apparatus or the spectrofluorometer depending on the mutated MsrA, as described in the previous section. The pH dependence of the reductase step rate constant for E94A and E94D MsrAs was determined under steady-state conditions using the Trx recycling system. k_{max} (or k_{obs}) values were plotted against pH and fitted to Equation 8, deriving from a

Downloaded from http://www.jbc.org/ at CNRS on January 23, 2018

one-pK_a model, where $k_{max\ opt}$ represents the maximum pH-independent rate constant.

$$k_{max} = \frac{k_{max\ opt}}{(1 + 10^{(pK_a - pH)})} \quad \text{(Eq. 8)}$$

RESULTS

Determination of pK_{app} of the Cys Residues

The pK_{app} of both Cys-51 and Cys-198 were determined in the reduced free enzyme by two methods. The first one involved determining the second-order rate constant of the reaction with the Cys-specific reactivity probe 2-PDS as a function of pH. The second one took advantage of the variation of the thiolate UV absorbance as a function of pH.

Kinetics of Reaction of Reduced Wild-type, C51S, and C198S MsrAs with 2PDS—Reaction of 2PDS with wild-type MsrA obeyed pseudo-first-order kinetics, with formation of 2 mol of pyridine-2-thione/mol of MsrA as determined from the absorbance change at 343 nm. This result was expected as two Cys are present in *N. meningitidis* MsrA at positions 51 and 198. For all pH used, stopped-flow traces fitted to monoexponential Equation 1, with amplitude corresponding to the release of 2 mol of pyridine-2-thione. pH-k_2 profile fitted to monosigmoidal Equation 2 with a pK_{app} value of 9.7 and k_{2max} value of $(2.4 \pm 0.3)\cdot10^5\ M^{-1}\ s^{-1}$ (Fig. 1*A*). The product of 2PDS reaction with wild-type MsrA is the disulfide-oxidized enzyme and not the thiopyridine adducts. Indeed, no release of pyridine-2-thione was observed when 10 mM dithiothreitol was added to the purified product (data not shown).

C51S and C198S MsrAs behaved similarly to wild-type MsrA, except that only 1 mol of pyridine-2-thione/mol of MsrA was formed. pK_{app} value of 9.3 ± 0.1 and a k_{2max} value of $(3.1 \pm 0.7)\cdot10^4\ M^{-1}\ s^{-1}$ for Cys-51 and a pK_{app} of 9.8 ± 0.1 and a k_{2max} value of $(2.6 \pm 0.6)\cdot10^4\ M^{-1}\ s^{-1}$ for Cys-198 were determined (Fig. 1*B*). Altogether, the data support a pK_{app} value of both Cys-51 and Cys-198 in the reduced free wild-type enzyme close to 9.5.

Direct Thiolate UV Absorbance of Reduced Wild-type, C51S, and C198S MsrAs—The thiolate absorbance of wild-type, C51S, and C198S MsrAs was monitored between pH 6 and 10. Analysis of the spectra and of the ϵ240 nm as a function of pH yielded monosigmoidal plots for all three MsrAs. Data fitted to pK values of 9.7, 9.8, and 9.7, associated with $\Delta\epsilon$240 nm of $3.1\cdot10^4$, $2.3\cdot10^4$, and $2.6\cdot10^4\ M^{-1}\cdot cm^{-1}$ for wild-type, C51S, and C198S MsrAs, respectively (Fig. 2). These pK_{app} values of Cys-51 and Cys-198 in the reduced free enzyme are in good agreement with those obtained with 2PDS.

Kinetic Characterization with Identification of the Rate-limiting Step of the Mutated MsrAs at pH 8

Steady-state catalytic constants of mutated MsrAs at positions 82, 94, and/or 134 were determined at pH 8, which is the optimum pH for the wild type (1). AcMetSONHMe was used instead of MetSO because MsrA displays a better affinity for AcMetSONHMe (9). As shown in Table 1, Y82F, Y134F, and E94Q MsrAs exhibited slight modifications of k_{cat} compared with wild-type MsrA, with k_{cat} values from 0.9 to 2.2 s^{-1} and a K_m increase from 0.8 to 25 mM. In contrast, E94A, E94D, Y82F/Y134F, and Y82F/Y134F/E94Q MsrAs showed strongly decreased k_{cat} values, from $1\cdot10^{-3}$ to $2.5\cdot10^{-1}\ s^{-1}$ and increased K_m from 24 to 161 mM.

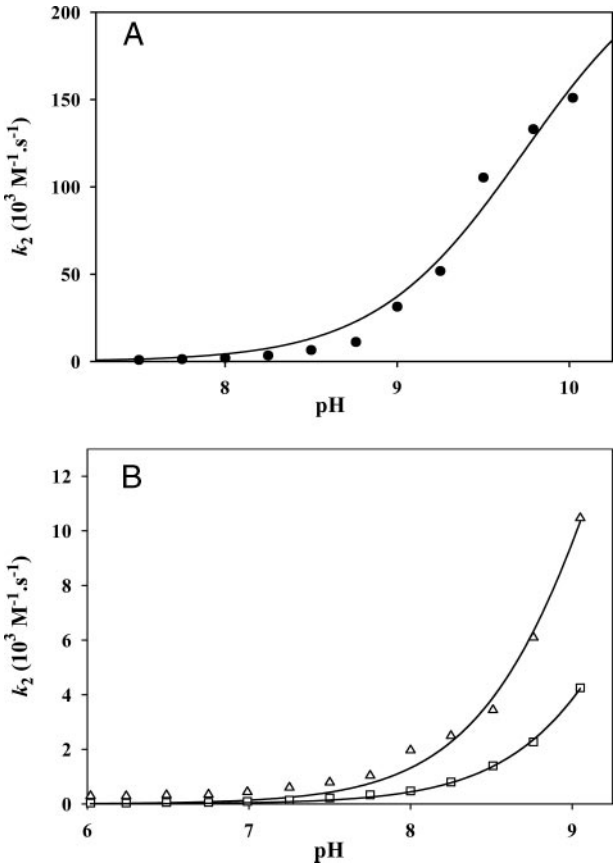

FIGURE 1. **pH dependence of the second-order rate constant k_2 for the reaction of the thiol group with 2PDS of wild-type (●, *panel A*), C51S (□, *panel B*) and C198S (Δ, *panel B*) MsrAs.** Reaction kinetics were performed at 25 °C over a pH range of 5–9 or 10 in polybuffer B. The concentrations of enzymes and 2PDS were 6.2 and 310 μM, respectively. Values of k_{obs} were determined using nonlinear regression analysis, and second-order rate constants k_2 were fitted to Equation 2 (*solid line*) (see also "Experimental Procedures"). The plateau of the sigmoidal plot was not attained at the pH tested. Therefore, the pK_{app} values obtained by fitting could only be taken as estimates.

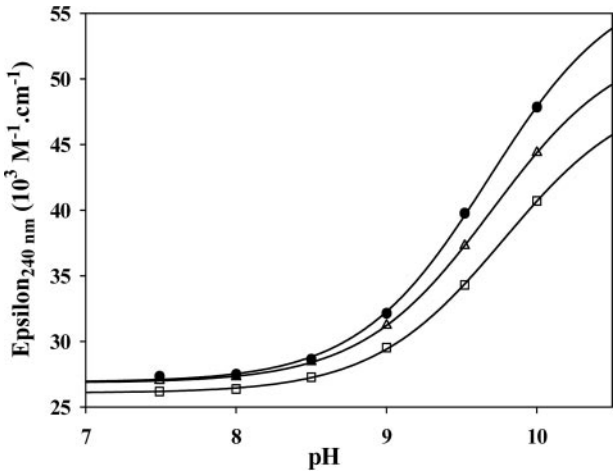

FIGURE 2. **pH dependence of the Cys thiol group absorbance properties of wild-type (●), C51S (Δ), and C198S (□) MsrAs.** Molecular absorption coefficients at 240 nm were calculated from the absorbance spectra from 300 to 200 nm performed over a pH range of 7 to 10 in polybuffer B. Absorption coefficients were fitted to Equation 3 (*solid line*) (see also "Experimental Procedures").

Downloaded from http://www.jbc.org/ at CNRS on January 23, 2018

TABLE 1

Steady-state and reductase step kinetic parameters of wild-type and mutated MsrAs, with associated pK_{app}

	Steady-state[a]		Reductase step			
	k_{cat}	K_m	k_{max}[b]	K_S[b]	$k_{max\ opt}$[c]	pK_{app}[c]
	s^{-1}, pH 8.0	*mM, pH 8.0*	*s^{-1}, pH 8.0*	*mM, pH 8.0*	*s^{-1}, optimal pH*	
Wild type	3.7 ± 0.5	0.6 ± 0.2	790 ± 10	55 ± 2	730 ± 10	5.7 ± 0.1
E94A	(1.5 ± 0.1)·10^{-2}	119 ± 27	(1.5 ± 0.1)·10^{-2}	119 ± 27	(2.0 ± 0.1)·10^{-2}	7.5 ± 0.1
E94D	0.25 ± 0.03	161 ± 42	0.25 ± 0.03	161 ± 42	0.19 ± 0.01	6.7 ± 0.1
E94Q	0.88 ± 0.07	25 ± 6	12.2 ± 0.3	151 ± 8	28 ± 3	8.0 ± 0.1
Y82F	2.2 ± 0.1	3.7 ± 0.7	51 ± 1	72 ± 4	46 ± 1	7.6 ± 0.1
Y134F	1.5 ± 0.1	0.8 ± 0.2	250 ± 8	70 ± 10	380 ± 10	7.7 ± 0.1
Y82F/Y134F	(1.5 ± 0.1)·10^{-2}	24 ± 8	(3.4 ± 0.1)·10^{-2}	26 ± 2	(7.2 ± 0.7)·10^{-2}	8.0 ± 0.1
Y82F/Y134F/E94Q	(1.0 ± 0.1)·10^{-3}	62 ± 22	(1.2 ± 0.1)·10^{-3}	28 ± 7	(1.1 ± 0.1)·10^{-2}	9.5 ± 0.1

[a] Steady-state parameters were deduced from nonlinear regression of initial rates to the Michaelis-Menten relationship (see "Experimental Procedures").
[b] Kinetic parameters of the reductase step were obtained from nonlinear regression of k_{obs} to Equation 7 (see "Experimental Procedures"), except for E94A and E94D MsrAs. For these two latter substituted MsrAs, k_{max} and K_S values correspond to k_{cat} and K_m values determined under steady-state conditions (see "Results").
[c] Kinetic parameters, $k_{max\ opt}$ at optimum pH and pK_{app} values, were deduced from nonlinear regression of k_{obs} to Equation 8 (see also Fig. 4).

In the wild type, the rate of the reductase step is largely higher than the k_{cat} value (1). Therefore, to interpret the eventual kinetic consequences of the substitutions at positions 82, 94, and 134 at the level of the reductase step, it was first necessary to attain this rate. This was determined for E94Q, Y82F, Y134F, Y82F/Y134F, and Y82F/Y134F/E94Q MsrAs by following the variation of the Trp-53 fluorescence intensity under single turnover conditions, *i.e.* in the absence of reductant (1). In that context, it was assumed that the reductase step of the mutated MsrAs is still rate-determining in the process leading to formation of the Msr disulfide bond,[4] as previously shown for the wild type (1). In the case of E94Q, Y82F, and Y134F MsrAs, formation of the disulfide bond led to an increase in the Trp-53 fluorescence emission similar to that described for the wild type, whereas a quenching of the fluorescence was observed for Y82F/Y134F and Y82F/Y134F/E94Q MsrAs.Structural factors responsible for this different behavior remain unknown. For all mutated MsrAs, the variation of the fluorescence signal in function of time is of monoexponential type whatever the AcMetSONHMe concentration. The kinetic parameters k_{max} and K_S values are summarized in Table 1. No strong K_S effect was observed for any of the five mutated MsrAs (K_S values ranging from 26 to 151 mM). The k_{max} value for E94Q MsrA is still high compared with that of the wild type and is 14-fold higher than k_{cat} value, which is indicative of a rate-limiting step still associated with the Trx-recycling step. This is also the case for Y82F and Y134F MsrAs for which the k_{max} values are 23- and 160-fold higher than k_{cat} values, respectively. In contrast, drastic effects on k_{max}, *i.e.* at least 2·10^4-fold decrease, were observed for Y82F/Y134F and Y82F/Y134F/E94Q MsrAs. Moreover, k_{max} and k_{cat} values are similar, showing that the reductase step is the rate-limiting step.

The fact that the variation of the Trp-53 fluorescence message is, for unknown reasons, not of monoexponential type for E94A and E94D MsrAs (curve not shown) led us to use another method to attain the kinetics of the reductase step for these two mutated MsrAs. This method, which was already used for the wild type, consists of following the rate of formation of AcMetNHMe and of the Cys-51/Cys-198 disulfide bond under single turnover conditions, *i.e.* in the absence of Trx. This was done at a saturating concentration of 300 mM AcMetSONHMe. E94D analysis required the use of a rapid mixing apparatus, whereas E94A study was possible by manual mixing. Formation of 0.9 mol of AcMetNHMe/mol of enzyme was observed for both E94D and E94A MsrAs. Rate constant for AcMetNHMe formation (k_{Met}) was 0.27 s^{-1} and 2.9·10^{-2} s^{-1} for E94D and E94A MsrAs, respectively. The free thiol content profile fitted to a monoexponential model, with concomitant loss of Cys-51 and Cys-198 thiols, with rate constant (k_{SS}) of 0.31 s^{-1} and 4.10^{-2} s^{-1} for E94D and E94A MsrAs, respectively. The fact that k_{Met}, k_{SS}, and k_{cat} values are similar indicated that the reductase step is rate-limiting for both mutated MsrAs. Therefore, the K_m value determined under steady-state conditions represents the K_S value of the reductase step. As observed for the other mutated MsrAs, the K_S values are similar to that of the wild type (see Table 1).

pH Dependence of the Kinetic Parameters of the MetSO Reductase Step

The kinetic parameters k_{max} and K_S of the reductase step for the wild type were determined at different pH values by fluorescence stopped-flow spectroscopy under single turnover conditions, *i.e.* in the absence of Trx. The pH-k_{max} plot, presented in Fig. 3, exhibits a monosigmoidal profile governed by the contribution of an ionizable group of pK_{app} 5.7 ± 0.1 that must be deprotonated for efficient MetSO reduction. This ionized species is characterized by a $k_{max\ opt}$ value of 730 s^{-1}.

For E94Q, Y82F, Y134F, Y82F/Y134F, and Y82F/Y134F/E94Q MsrAs, the rate of the reductase step was also measured by fluorescence spectroscopy under single turnover conditions, either on a stopped-flow apparatus or a conventional spectrofluorometer, depending on the value of the rate. In the case of E94A and E94D MsrAs, the rate of the reductase step was determined under steady-state conditions. For each substituted MsrA, the observed rate constant k_{obs} of the MetSO reductase step was measured, at each pH, with only one concentration of AcMetSONHMe (300 mM). This concentration was shown to be saturating over the pH range investigated except for E94Q MsrA (data not shown). Therefore, k_{obs} value can be considered

[4] For each Glu-94-mutated MsrA, the rate constant of the reductase step was shown to be rate-determining in the two-step process leading to the formation of the disulfide bond by following the rate of AcMetNHMe and disulfide bond formation directly by acid-quenching of the reaction, followed by quantification of product and MsrA remaining free thiols (see "Results" for E94A and E94D MsrAs, data not shown for E94Q). For each Tyr-substituted MsrA, the rate of the reductase step was shown to be too fast at pH 8 to allow direct determination of the rate of AcMetNHMe and disulfide bond formation (data not shown).

Downloaded from http://www.jbc.org/ at CNRS on January 23, 2018

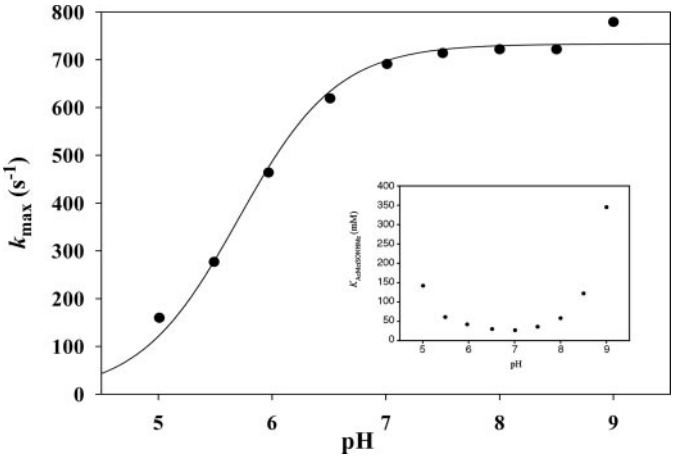

FIGURE 3. **pH dependence of the reductase step rate constant k_{max} and AcMetSONHMe affinity constant K_S (*inset*) of wild-type MsrA.** Kinetics of MsrA fluorescence variation were followed after excitation at 284 nm on a stopped-flow apparatus by rapidly mixing 10 μM enzyme and various concentrations of AcMetSONHMe (50–800 mM) at various pH values in polybuffer B. It should be noted that, below pH 5.5, disulfide bond formation is not accompanied by an increase but by a quenching of Trp-53 fluorescence emission for an unknown reason (curve not shown). For each pH, experimental k_{obs} data obtained at each substrate concentration were analyzed by nonlinear regression against Equation 7 to obtain k_{max} and K_S values (see also "Experimental Procedures"). k_{max} values (●) were plotted against pH and fitted to Equation 8 (*solid line*) leading to a $k_{max\ opt}$ value of 730 s^{-1} and pK_{app} value of 5.7.

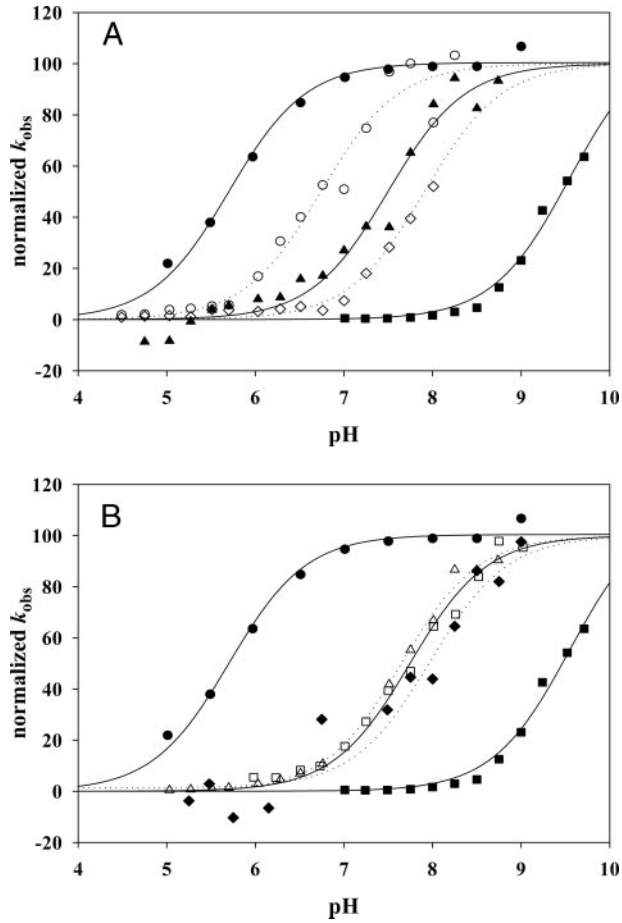

FIGURE 4. **pH dependence of the reductase step rate constant k_{max} of wild-type and substituted MsrAs.** For wild-type MsrA, refer to Fig. 3. For all substituted MsrAs, the rate of the reductase step was determined with 300 mM AcMetSONHMe at various pH values in polybuffer B. The independence of the rate constant on AcMetSONHMe concentration was verified at two extreme pH values (around 5 and 9). For E94Q, Y82F, and Y134F MsrAs, the increase of Trp-53 fluorescence intensity was followed after excitation at 284 nm on a stopped-flow apparatus. For Y82F/Y134F and E94Q/Y82F/Y134F MsrAs, variation of fluorescence emission was recorded on a spectrofluorometer with excitation and emission wavelength set at 284 and 340 nm, respectively. For E94A and E94D MsrAs, the reductase step rate constant was followed using the Trx-recycling system. Experimental k_{obs} data obtained at each pH were analyzed by nonlinear regression against Equation 8 to obtain $k_{max\ opt}$ and pK_{app} values (see also "Experimental Procedures"). $k_{max\ opt}$ and pK_{app} values are presented in Table 1. Experimental k_{obs} data were normalized, taking $k_{max\ opt}$ value as 100% for each enzyme, for the clarity of the representation. *Symbols* represent normalized data, and *lines* represent the fit. *Panel A*, wild type (●, *solid line*); E94A MsrA (▲, *solid line*); E94D MsrA (○, *dotted line*); E94Q MsrA (◇, *dotted line*); E94Q/Y82F/Y134F MsrA (■, *solid line*). *Panel B*, wild type (●, *solid line*); Y82F MsrA (□, *solid line*); Y134F MsrA (Δ, *dotted line*); Y82F/Y134F MsrA (◆, *dotted line*); E94Q/Y82F/Y134F MsrA (■, *solid line*).

as a k_{max} value. In the case of E94Q MsrA, 300 mM AcMetSONHMe was not saturating at pH >8, and consequently k_{obs} values were determined only up to pH 8. The k_{obs} profile remains monosigmoidal for all substituted MsrAs, with increasing k_{obs} value with increasing pH. Data fitted to a single pK_a model (see Fig. 4). E94D MsrA has a pK_{app} of 6.7 with a $k_{max\ opt}$ value of 0.19 s^{-1}. E94A, E94Q, Y82F, Y134F, and Y82F/Y134F MsrAs displayed a more pronounced pK_{app} shift, with values ranging from 7.5 to 8.0 and with $k_{max\ opt}$ values of $2{\cdot}10^{-2}$, 28, 46, 380, and $7{\cdot}10^{-2}$ s^{-1}, respectively (see Fig. 4 and Table 1). It is noteworthy that substitutions of Tyr-82 or Tyr-134 induced a similar pK_{app} shift to 7.6 and that double substitution of these two Tyrs led to a higher shift to 8.0. The triple substituted MsrA Y82F/Y134F/E94Q displayed the most highly shifted pK_{app}, with a value of 9.5 and the lowest $k_{max\ opt}$ value of $1.1{\cdot}10^{-2}$ s^{-1} (see Fig. 4 and Table 1).

DISCUSSION

The methionine sulfoxide reductase step of the MsrA mechanism was previously shown to be very fast (1) and postulated to imply the formation of a sulfurane transition state of bipyramidal geometry on the basis of the theoretical chemistry study (6). According to these data, the reductase step should imply 1) the formation of an enzyme-substrate complex, 2) the deprotonation of Cys-51, 3) the involvement of an acid catalyst to protonate the sulfoxide substrate and favor the sulfurane-type transition state formation, and 4) the rearrangement of the sulfurane-type transition state to obtain Met and sulfenic acid. The invariant residues Glu-94, Tyr-82, and Tyr-134 are correctly positioned in the three available x-ray MsrA structures to interact via H-bond with a water molecule that is located at the place of the oxygen of the sulfoxide function (Fig. 5). Based on these structural features, a reasonable hypothesis supports Glu-94 as the presumably required acid catalyst. This proposition is reinforced by the observation that no other acidic residue is present in the close proximity of the sulfoxide function. The two phenolic side chains of Tyr-82 and Tyr-134 could be involved in substrate binding (*i.e.* an affinity contribution) and/or in substrate positioning and transition state stabilization (*i.e.* a chemical catalysis contribution).

Cys-51 Activation within the Active Site—In the free wild-type enzyme, 2-PDS titration and direct thiolate UV absorbance titration revealed a single pK_{app} ~9.5 for both Cys-51 and -198. Moreover, the 2PDS chemical reactivity of MsrA Cys is

Downloaded from http://www.jbc.org/ at CNRS on January 23, 2018

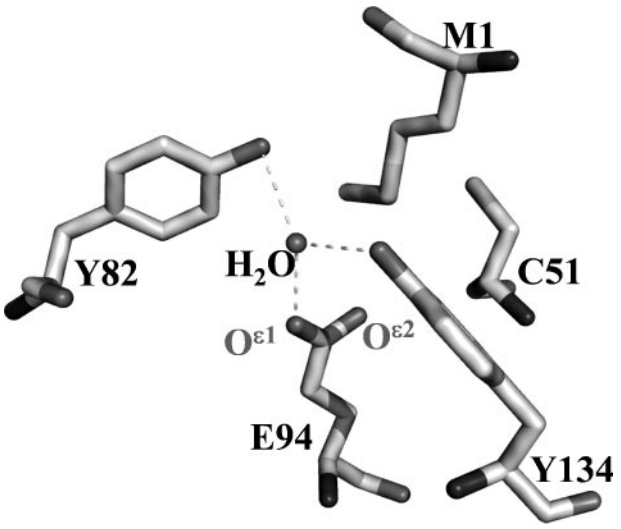

FIGURE 5. **Schematic representation of *M. tuberculosis* MsrA active site containing methionine 1 (*M1*) from a neighboring monomer (from Ref. 3).** Residues Cys-51, Glu-94, Tyr-82, and Tyr-134 are shown together with bound M1. The water molecule is also represented in the active site by a *sphere*. The *dashed lines* represent the hydrogen bonds observed between residues and the water molecule. Monitored distances between atoms are: $d(O^{\varepsilon1}_{E94}\text{-}O_{H2O})$ = 2.52 Å; $d(O^{\varepsilon2}_{E94}\text{-}S^{\delta}_{M1})$ = 3.43 Å; $d(O^{\varepsilon2}_{E94}\text{-}S^{\gamma}_{C51})$ = 5.06 Å; $d(S^{\gamma}_{C51}\text{-}S^{\delta}_{M1})$ = 3.47 Å; $d(O^{\zeta}_{Y82}\text{-}O_{H2O})$ = 2.88 Å; $d(O^{\zeta}_{Y82}\text{-}S^{\delta}_{M1})$ = 3.57 Å; $d(O^{\zeta}_{Y134}\text{-}O_{H2O})$ = 2.75 Å, $d(O_{H2O}\text{-}S^{\delta}_{M1})$ = 3.33 Å; $d(O^{\zeta}_{Y82}\text{-}S^{\gamma}_{C51})$ = 6.61 Å; $d(O^{\zeta}_{Y134}\text{-}S^{\gamma}_{C51})$ = 7.16 Å.

comparable with that of the thiolate of glutathione (10), arguing for two Cys residues not activated but accessible in the free wild-type MsrA. The fact that 2PDS mediates oxidation of reduced MsrA to its disulfide state with simultaneous liberation of two moles of pyridine-2-thione/enzyme, via an apparent one-step kinetic mechanism, can be explained by a mechanism reminiscent of that of the Msr mechanism. First, the rate-limiting reaction between one Cys and one molecule of 2PDS would lead to a transient mixed disulfide. This disulfide would be rapidly attacked by the second Cys of the enzyme, leading to the disulfide-oxidized MsrA. Such a mechanism would imply that the measured pK_{app} only reflects ionization of the first Cys. It is tempting to assign Cys-51 as this "2-PDS-reactive" Cys. 2-PDS titration of C51S and C198S MsrAs supports this assignment, as Cys-51 (C198S MsrA) exhibits a stronger reactivity than Cys-198 (C51S MsrA) between pH 8 and 9 (see Fig. 1*B*). The measured pK_{app} values around 9.5 for Cys-51 and Cys-198, respectively, are significantly higher than the value of 8.8 for the model Cys of glutathione (10). As MsrA function is supposed to be widely used during oxidative stress burst, high pK_a could serve as a protection against oxidative modification of both Cys by restricting their reactivity toward reactive oxygen or nitrogen species. Stabilization of the thiol state of Cys-51 could be provided by the hydrophobic character of the active site.

As stated above, Cys-51 has to be deprotonated to allow its efficient attack on the sulfoxide function. The observed high rate constant of the reductase step at pH 8.0 implies a large, mandatory shift in Cys-51 pK_a, from near 9.5 to at least somewhere below 7. The pH dependence of k_{max} displays a single pK_{app} of 5.7, the rate of sulfoxide reduction increasing with pH. Moreover, the E94Q and Y82F/Y134F/E94Q MsrAs still show the contribution of a single p*K* of 8 and 9.5, respectively. Such results support the attribution of the pK_{app} of 5.7 to Cys-51 and not to Glu-94. Thus, formation of the MsrA-AcMetSONHMe complex provokes an activation of Cys-51 by decreasing its pK_{app} by 3.8 units.

Glu-94, Tyr-82, and Tyr-134 Contributions in the Reductase Step—Substitution of Glu-94 by Ala or Asp drastically decreased the $k_{max\ opt}$ rate of the reductase step of the MsrA mechanism by factors of $3.6 \cdot 10^4$ and $3.8 \cdot 10^3$, respectively, with no significant K_S effect at pH 8 and caused the shift of the rate-limiting step from the Trx-recycling process to the sulfoxide reduction step. These data support the implication of Glu-94 in the catalysis of sulfoxide reduction, but not in substrate binding, and identify its side chain as a critical catalyst. However, the kinetic parameters of the reductase step obtained with E94Q MsrA revealed a rather minor $k_{max\ opt}$ decrease of only 26-fold compared with that of the wild type. As Gln-94 cannot be a proton donor, it is tempting to conclude that Glu-94 does not directly play a role as general acid catalyst but likely stabilizes, via H-bonding, the sulfurane transition state leading to sulfenic acid formation (see the last paragraph under "Discussion"). Indeed, substitution of Glu by Gln retains an H-bonding ability. This is reinforced by the fact that no pK_{app} of an acidic catalyst is observed on the pH-k_{max} profile of the wild-type MsrA. In addition to this effect on the rate constant of the sulfoxide reduction, substitution of Glu-94 induced an increase of the pK_{app} governing this step and assigned to Cys-51. Thus, Glu-94 is, directly or not, also involved in the activation of Cys-51 upon substrate binding.

Substitution of Tyr-82 and Tyr-134, or both, by Phe did not affect K_S values. Moreover, the $k_{max\ opt}$ constant of the sulfoxide reduction was slightly decreased by the absence of one of the phenolic hydroxyls, in particular of Tyr-134, but drastically decreased when both were removed. The fact that substitutions of both Tyrs is required to observe a strong decrease of $k_{max\ opt}$ suggests that in single Tyr-substituted MsrA the remaining Tyr in the presence of Glu-94 compensates the absence of the second phenolic hydroxyl. Similarly to Glu-94, substitution of Tyr-82 and/or Tyr-134 also leads to an increase of the pK_{app} governing this step, assigned to Cys-51. Importantly, in contrast to the catalytic role of Tyr-82 and Tyr-134, which can be fairly well assumed by only one Tyr, Cys-51 activation is more sensitive to the absence of one of the two phenolic side chains.

Taken together, these data strongly suggest that Glu-94, Tyr-82, and Tyr-134, in addition to their role in favoring the polarized form of the sulfoxide function of the substrate bound, are involved in the stabilization of the sulfurane transition state (see the last paragraph under "Discussion") that precedes the sulfenic acid formation. They also participate, directly or indirectly, in the Cys-51 activation upon formation of the MsrA-substrate complex. As a confirmation, the triple substituted MsrA Y82F/Y134F/E94Q displays the most highly shifted pK_{app} with a value of 9.5, close to the pK_{app} of Cys-51 determined in the free enzyme, and the biggest reduction of $k_{max\ opt}$, by a factor of $6.6 \cdot 10^4$ compared with the wild type.

Structure/Function Relationships within the MsrA Active Site—The available x-ray structure of MsrA from *M. tuberculosis* in complex with a Met from a neighboring monomer pro-

Downloaded from http://www.jbc.org/ at CNRS on January 23, 2018

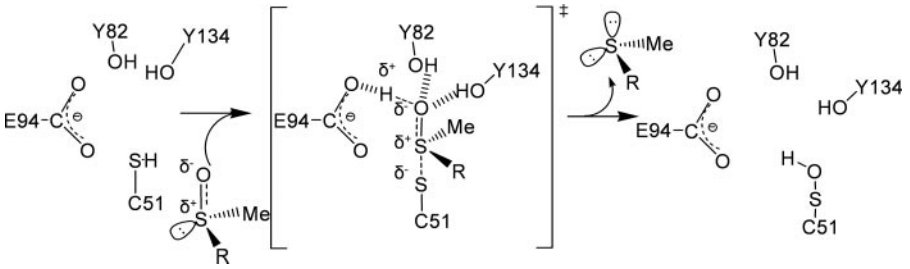

SCHEME 2. **Schematic representation of the catalytic mechanism of the MetSO reductase step of MsrA from *N. meningitidis*.** The four essential functional groups of Cys-51, Glu-94, Tyr-82, and Tyr-134 are represented. $RSOCH_3$ and $RSCH_3$ represent MetSO and Met, respectively. The substrate binds to the active site with its sulfoxide function largely polarized. A transition state (or intermediate) of sulfurane type is then likely formed as proposed from theoretical computations (6). The nature of the rearrangement that leads to formation of the sulfenic acid intermediate and of Met remains to be determined. See "Discussion" for more details on the mechanism.

vides a good model of the substrate-MsrA complex (3). Inspection of the structure shows that no residue bearing a positively charged side chain is present in close proximity to Cys-51 (Fig. 5). Moreover, on one hand the distance between the carboxylate of Glu-94 and the sulfur atom of Cys-51 (5.1 Å) is by far too large to allow a direct interaction between these two functions. On the other hand, the sulfur atom of the Met residue is positioned between one oxygen atom of the carboxylate and the thiol function of Cys-51. Thus, stabilization of the thiolate form of Cys-51 by the protonated form of Glu-94 is rather unlikely. The direct implication of Tyr-82 and Tyr-134 is also unlikely, as the distance between their hydroxyl groups and the thiol of Cys-51 is too large (at least 6.6 Å, Fig. 5). Therefore, the decrease in pK_{app} of 3.7 units of Cys-51 in the Michaelis complex is likely due to a substrate-assisted mechanism. In the MsrA-substrate complex, the polarization of the sulfur-oxygen bond should be favored by the presence of the side chains of Glu-94, Tyr-82, and Tyr-134. Such a polarization was already described for the sulfur-oxygen bond of the Me_2SO by using theoretical chemistry method (11–13) and experimental approaches that gave a dipole moment of 3.96 D (14, 15). The close proximity of a positive, or a partially positive, charge on the sulfur of the sulfoxide function near the thiol group of Cys-51 (3.4 Å between the sulfur of Met and the thiol of Cys-51 in the *M. tuberculosis* binary complex MsrA-Met, Fig. 5) likely stabilizes the thiolate form of Cys-51 and thus is believed to be the driving force that favors the shift of the Cys-51 pK_a from 9.5 to 5.7 upon substrate binding. In the case of the E94Q MsrA, the same scenario occurs but the polarization of the sulfur-oxygen bond could be lesser developed, leading to a smaller positive partial charge on the sulfur atom and therefore to the shift of the Cys-51 pK_{app} from 5.7 to 8. It is likely that the proton initially borne by Cys-51 is transferred to the oxygen of the sulfoxide function via a concerted mechanism concomitantly with the attack of the thiolate of Cys-51 on the sulfoxide sulfur atom, leading to the formation of the sulfurane-type transition state. In this context, a proton shift that transfers the proton coming from the thiol of Cys-51 to the oxygen of the sulfoxide must occur. It is seductive to postulate that this proton transfer could be catalyzed via Glu-94. However, as already mentioned, in the structure of *M. tuberculosis* MsrA, the distance of 5.1 Å between the thiol of Cys-51 and the nearest oxygen of Glu-94 is too far for a direct interaction unless a shortening of this distance occurs or a water molecule is transiently present between the carboxylate and the thiol.

Proposed Scenario for the Sulfoxide Reductase Step of the MsrA Mechanism—MetSO likely binds to the active site of MsrA with its sulfoxide largely in its polarized form. The spatial proximity between the sulfur of the sulfoxide function and the thiol of Cys-51 leads to a stabilization of the thiolate form due to the presence of the positive, or partially positive, charge borne by the sulfur. Concomitantly to the substrate binding, the proton of Cys-51 is transferred to the oxygen of the sulfoxide function and the positively, or partially charged, sulfur of MetSO undergoes a nucleophilic attack of the Cys-51 thiolate leading to the formation of a sulfurane transition state of trigonal bipyramidal geometry, as suggested from quantum chemistry calculations (6) (see Scheme 2). How the rearrangement occurs for forming the sulfenic acid intermediate and Met remains to be determined. The mechanism is likely concerted rather than stepwise. In this scenario, Glu-94, Tyr-82, and Tyr-134 have two roles. First, they favor the binding of the polarized form of the sulfoxide function that is the form that is also present in solution. Second, they stabilize the sulfurane transition state. In that context, Glu-94 has the most important contribution and probably intervenes under its carboxylate form, whereas Tyr-82 and Tyr-134 form a hydrogen bond with the two lone pairs of the hydroxyl group.

However, questions remain to be addressed on the mechanism that allows the formation of a sulfenic acid of tetrahedral geometry from a sulfurane transition state of trigonal bipyramidal geometry. Indeed, recent theoretical study of the reduction mechanism of Me_2SO by thiols supports the formation of a sulfurane transition state with the sulfur of the thiol and the OH group in apical position and the two methyl groups and the lone pair in equatorial position (6). Such a geometry is, however, not compatible with a direct shift of the OH group to the sulfur atom of the thiol. A possibility that has also been considered is the formation of a transition state with the sulfur of the thiol into equatorial position and the OH group into apical position. The S–S–O bond angle is near 90°. Such a geometry necessitates higher activation energy to attain the transition state (~20 kcal/mol) that leads to shift of the OH group to the thiol group (6). An alternative that has also been proposed is to form a transition state of epoxide type. In that case, the geometry is more favorable to a shift of the OH group to the thiol group but the penalty in terms of energy of activation is higher (~40 kcal/mol) (6). Another question concerns the way by which the proton of the sulfur of Cys-51 is transferred to the sulfoxide function. An evident candidate is Glu-94. However, as already pointed out, the distance between Cys-51 and Glu-94 is at least 5 Å. In this context, the studies that are underway by theoretical approaches and taking into account the structure of the MsrA active site will be of particular interest.

Downloaded from http://www.jbc.org/ at CNRS on January 23, 2018

Acknowledgments—We thank Prof. W. W. Cleland, Dr. M. F. Ruiz-Lopez, and Dr. G. Monard for helpful discussions. We thank Dr. F. Barras for the kind gift of the BE002 E. coli strain, C. Gauthier and A. Kriznik for their very efficient technical help and AcMetSONHMe synthesis, Dr. G. Chevreux and Dr. S. Sanglier-Cianferani for mass spectrometry analysis, and Dr. S. Sonkaria for reviewing the manuscript.

REFERENCES

1. Antoine, M., Boschi-Muller, S., and Branlant, G. (2003) *J. Biol. Chem.* **278,** 45352–45357
2. Olry, A., Boschi-Muller, S., and Branlant, G. (2004) *Biochemistry* **43,** 11616–11622
3. Taylor, A. B., Benglis, D. M., Jr., Dhandayuthapani, S., and Hart, P. J. (2003) *J. Bacteriol.* **185,** 4119–4126
4. Tete-Favier, F., Cobessi, D., Boschi-Muller, S., Azza, S., Branlant, G., and Aubry, A. (2000) *Structure Fold Des.* **8,** 1167–1178
5. Lowther, W. T., Brot, N., Weissbach, H., and Matthews, B. W. (2000) *Biochemistry* **39,** 13307–13312
6. Balta, B., Monard, G., Ruiz-Lopez, M. F., Antoine, M., Gand, A., Boschi-Muller, S., and Branlant, G. (2006) *J. Phys. Chem. A* **110,** 7628–7636
7. Olry, A., Boschi-Muller, S., Marraud, M., Sanglier-Cianferani, S., Van Dorsselear, A., and Branlant, G. (2002) *J. Biol. Chem.* **277,** 12016–12022
8. Boschi-Muller, S., Azza, S., Sanglier-Cianferani, S., Talfournier, F., Van Dorsselear, A., and Branlant, G. (2000) *J. Biol. Chem.* **275,** 35908–35913
9. Boschi-Muller, S., Olry, A., Antoine, M., and Branlant, G. (2005) *Biochim. Biophys. Acta* **1703,** 231–238
10. Marchal, S., and Branlant, G. (1999) *Biochemistry* **38,** 12950–12958
11. Dobado, J. A., Martinez-Garcia, H., Molina, J. M., and Sundberg, M. R. (1999) *J. Am. Chem. Soc.* **121,** 3156–3164
12. Stener, M., and Calligaris, M. (2000) *J. Mol. Struct. (Theochem.)* **497,** 91–104
13. Mrazkova, E., and Hobza, P. (2003) *J. Phys. Chem. A* **107,** 1032–1039
14. Cotton, F. A., and Francis, R. (1960) *J. Am. Chem. Soc.* **82,** 2986–2991
15. Dreizler, H., and Dendl, G. (1964) *Z. Naturforsch.* **19a,** 512–514

Downloaded from http://www.jbc.org/ at CNRS on January 23, 2018

Characterization of the Amino Acids from *Neisseria meningitidis* MsrA Involved in the Chemical Catalysis of the Methionine Sulfoxide Reduction Step

Mathias Antoine, Adeline Gand, Sandrine Boschi-Muller and Guy Branlant

J. Biol. Chem. 2006, 281:39062-39070.
doi: 10.1074/jbc.M608844200 originally published online October 24, 2006

Access the most updated version of this article at doi: 10.1074/jbc.M608844200

Alerts:
- When this article is cited
- When a correction for this article is posted

Click here to choose from all of JBC's e-mail alerts

This article cites 15 references, 4 of which can be accessed free at
http://www.jbc.org/content/281/51/39062.full.html#ref-list-1

Downloaded from http://www.jbc.org/ at CNRS on January 23, 2018